Nonlinear Phenomena in Complex Systems, vol. **12**, no. 1 (2009), pp. 37 - 45

Some Aspects of Chaotic Lasing in Volume Free Electron Lasers

S. N. Sytova*
Research Institute for Nuclear Problem, Belarusian State University,
11 Bobruiskaya Str., 220030 Minsk, BELARUS
(Received 25 November, 2008)

Chaotic dynamics in Volume Free Electron Lasers (VFEL) is excited by significant perturbation in movement of electrons through resonator and by deformation of bunches leading to generation of higher harmonics in the system and vice versa. Analysis of phase electron dynamics are presented to explain origin of chaos in VFEL. Investigations presented are attempts to display origin of steady-state stationary and oscillatory VFEL regimes and demonstrate structure of electron bunches originating when electron beam passing through photonic crystal in VFEL.

PACS numbers: 41.60.Cr; 35Q60, 35F20, 65M06
Keywords: Volume Free Electron Laser, mathematical modelling, chaos

1. Physical principles of VFEL

We consider interaction of relativistic electron beams with three-dimensional periodical structures in Volume Free Electron Lasers (VFEL).

The main principle of vacuum electronic devices such as travelling wave tubes (TWT), backward wave tubes (BWT) [1], [2], free electron lasers (FEL) [3] is based on radiation of bunches of charged particles moving over the surface or through the slow-wave system (resonator). Under conditions of synchronism they begin to transform kinetic energy of charged particles to energy of electromagnetic radiation. In TWT, BWT, orotrons and other analogous devices a ribbon-like or annular electron beam is used. This is explained by the fact that the effective distance d of beam interaction with the surface of the slow-wave system is determined by the following formula: $d = \frac{\lambda\beta\gamma}{4\pi}$, where γ is the Lorentz factor of electron beam, $\beta = u/c$, u is a beam velocity, c is velocity of light. If e.g. we estimate the wave length as $\lambda = 1$ cm and $\beta = 0.8$, then we obtain $d \sim 0.1$ cm. This leads to significant restriction on device power.

Moreover in considered types of devices an interaction of moving forward electrons in a bunch with a stream of energy of electromagnetic waves occurs usually under one-dimensional distributed feedback. I.e. electrons in bunches and electromagnetic waves spread along one straight line: in one direction or in opposite directions. Here an estimation for the beam threshold current is the next [1], [3]:

$$j_{start} \sim \frac{1}{(kL)^3}, \tag{1}$$

where k is a wave number, L is a resonator length.

The new law of instability for an electron beam passing through a spatially-periodic target under diffraction in degeneration points were proposed in [4], [5]. There is shown that the increment of such instability increases essentially in comparison with the single-wave system. Analogous to (1) estimation in this case is the following:

$$j_{start} \sim \frac{1}{(kL)^{3+2s}},$$

where s is a number of surplus waves appearing in the system because of diffraction. This means the noticeable reduction of electron beam current

*E-mail: sytova@inp.minsk.by

density necessary for achievement the generation threshold in comparison with other devices and feasibility of resonator miniaturization.

Established physical mechanism [4], [5] is universal and valid for all wavelength ranges regardless the spontaneous radiation mechanism. On these physical principles a new type of electronic devices was proposed to create [5]-[7]. Its name is Volume Free Electron Laser. The basic difference of VFEL from different types of electronic devices is the availability of volume (non-one-dimensional) distributed feedback when an electron beam and some strong coupled electromagnetic waves spread angularly one to other in the system under diffraction in degeneration points. By assignment of system parameters VFEL can operate in regimes of TWT or BWT. Moreover in VFEL there is no restriction on using broad (in cross-section) electron beams.

As a slow-wave system (a spatially-periodic resonator) natural crystals for X-ray wavelength range [6] or artificial structures (so-called photonic crystals) for other ranges [7], [8] can be used.

First lasing of VFEL in mm wavelength range obtained recently [9]. Further experimental VFEL investigation is continued in cm wavelength [10], [11].

Common scheme of two-wave VFEL is depicted in Fig.1. Here an electron beam with electron velocity $\mathbf{u}$ and electron density n_b passes through a photonic crystal of the length L. Under diffraction conditions two strong electromagnetic waves can be excited in the resonator. If simultaneously electrons are under synchronism condition, they emit electromagnetic radiation in directions depending on diffraction conditions.

2. VFEL basic equations

The linear stage of interaction of electron beams with periodical structures investigated analytically [5], [6] quickly changes into the nonlinear one where most of the electron beam energy is transformed into electromagnetic radiation. System of equations describing such an interaction is obtained from Maxwell equations in the slowly-varying envelope approximation.

Let us consider two-wave geometry depicted in Fig.1. Electric field strength $\mathbf{E}$ and electron beam current density $\mathbf{j}$ are considered in the form:

$$\begin{aligned} &\mathbf{E} = \mathbf{e}_\sigma (E e^{i(\mathbf{kr}-\omega t)} + E_\tau e^{i(\mathbf{k}_\tau \mathbf{r}-\omega t)}), \\ &\mathbf{j} = \mathbf{e}_\sigma j e^{i(\mathbf{kr}-\omega t)}. \end{aligned} \tag{2}$$

Here $\mathbf{e}_\sigma$ is a vector of sigma polarization [12], ω is a frequency. τ is a reciprocal lattice vector. $\mathbf{k}$, $\mathbf{k}_\tau = \mathbf{k} + \tau$ are wave vectors of electromagnetic waves that are under diffraction conditions:

$$2k_z\tau_z \approx -2\mathbf{k}_\perp\tau_\perp + \tau^2.$$

Electromagnetic wave with vector $\mathbf{k}$ is called transmitted and one with vector $\mathbf{k}_\tau$ is diffracted. E and E_τ are complex-valued amplitudes of these waves.

It was proposed here that the electron beam is synchronous with the transmitted wave E only. This means the following synchronism condition is fulfilled:

$$|\omega - \mathbf{ku}| \le \delta\omega,$$

where δ is detuning from exact synchronism condition.

So, we obtain the following system of equations describing electromagnetic field dynamics in VFEL:

$$\begin{aligned} &\frac{\partial E}{\partial t} + \gamma_0 c\frac{\partial E}{\partial z} + 0.5i\omega l E - 0.5i\omega\chi_\tau E_\tau = I, \\ &\frac{\partial E_\tau}{\partial t} + \gamma_1 c\frac{\partial E_\tau}{\partial z} + 0.5i\omega\chi_{-\tau} E - 0.5i\omega l_1 E = 0. \end{aligned} \tag{3}$$

Here γ_0, γ_1 are distributed feedback cosines having form $\gamma_0 = \frac{k_z}{k}$, $\gamma_1 = \frac{k_{\tau z}}{k}$, $l = l_0 + \delta$, $l_{0,1} = \left(k_{,\tau}^2 c^2 - \omega^2\varepsilon_0\right)/\omega^2$. $\epsilon_0 = 1+\chi_0$, $\chi_0, \chi_{\pm\tau}$ are Fourier components of the dielectric susceptibility of resonator. Right-hand side I in (3) is described below.

Initial and boundary conditions for the system (3) depends on coupled waves directions

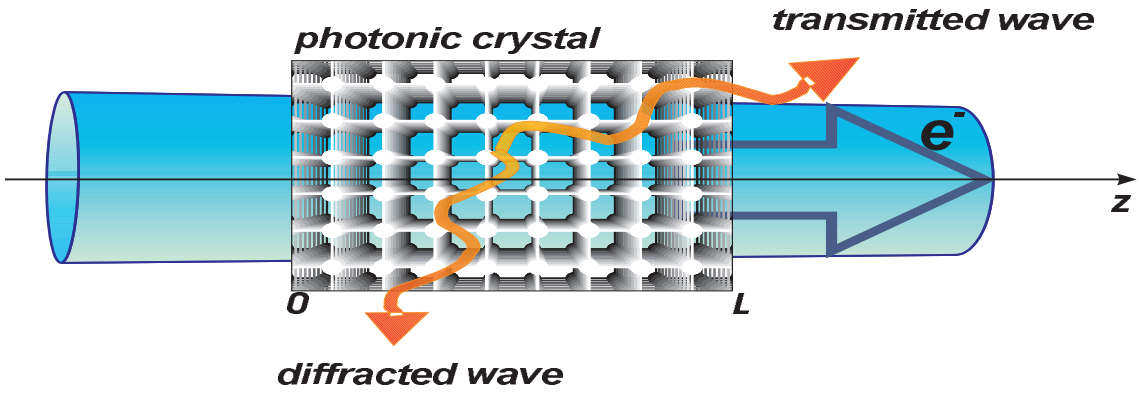

FIG. 1: Two-wave VFEL.

and can have different forms including external reflectors. Their simplest form is the following:

$$E(t, z = 0) = E_0, \quad E_\tau(t, z = L) = 0, \qquad E(t = 0, z) = 0, \quad E_\tau(t = 0, z) = 0. \tag{4}$$

System (3)–(4) must be supplemented by equations of phase dynamics of electron beam.

Let us use the method of averaging over initial phases of electrons that is well-known [2] and widely used in simulation of electronic vacuum devices [13]. We consider magnetized electron beam which propagation can be considered as one-dimensional. We introduce function $\Theta(t, z, p)$ describing the phase of electron beam relative to electromagnetic field. Moreover let us take into consideration as initial phase of an electron not only the moment of time t_0 of an electron entrance in resonator at $z = 0$ but also transverse spatial coordinate in this moment. In simulation of TWT, BWT etc. (see e.g. [13]) because of considering ribbon-like electron beams there is no necessity to take into account transverse spatial coordinate of an electron entrance in the slow-wave system. So, our approach is more complicated but it allows to simulate broad in cross-section electron beam dynamics.

Initial phase is an individual mark of the electron in the beam. Phase of each electron emerged in resonator at the moment t_0 can be presented as

$$\Theta(t, t_0, \mathbf{r}_\perp) = k_z z + \mathbf{k}_\perp \mathbf{r}_\perp - \omega t(z, t_0),$$

where $t(z, t_0)$ is a trajectory of electron passing through resonator. At its beginning $z = 0$ initial phase has the form:

$$\Theta(t = t_0, t_0, \mathbf{r}_\perp) = \mathbf{k}_\perp \mathbf{r}_\perp - \omega t_0 = \Theta_1 - \Theta_0 = p.$$

where $\Theta_0, \Theta_1 \in [0, 2\pi]$, $p \in [-2\pi, 2\pi]$. We consider below only combination of these initial phases $\Theta_1 - \Theta_0$. Averaging over this combination phase allows to pass from microscopical description to macroscopical one.

Motion equation for each electron has the form:

$$\frac{d\mathbf{p}}{dt} = e\left\{\mathbf{E} + \frac{1}{c}[\mathbf{v} \times \mathbf{H}]\right\}, \quad \mathbf{p} = m\gamma\mathbf{v},$$

where e and m are electron charge and mass respectively.

Performing some transformations and taking into account that

$$v = \frac{1}{\frac{dt}{dz}}, \quad \frac{dv}{dt} = -\frac{\frac{d^2t}{dz^2}}{\left(\frac{dt}{dz}\right)^3}, \quad \frac{dt}{dz} = -\frac{1}{\omega}\left(\frac{d\Theta}{dz} - k_z\right)$$

we obtain finally:

$$\frac{d^2\Theta}{dz^2} = \frac{e\Phi}{m\gamma^3\omega^2}\left(k_z - \frac{d\Theta}{dz}\right)^3 \cdot \mathrm{Re}\left(Ee^{i\Theta}\right), \qquad \frac{d\Theta(t, 0, p)}{dz} = k_z - \omega/u, \quad \Theta(t, 0, p) = p, \tag{5}$$

where $\Phi = \sqrt{l_0 + \chi_0 - 1/(\beta\gamma)^2}$.

In (3)–(5) $t > 0$, $z \in [0, L]$, $p \in [-2\pi, 2\pi]$.

Let us determine right-hand side of (3) I. From Maxwell equations using (2) it is the next

$$I = -\frac{2\pi i}{\omega}\left(\mathbf{e}_\sigma \frac{\partial \mathbf{j}}{\partial t}\right) e^{-i(\mathbf{kr}-\omega t)}. \qquad (6)$$

Beam current can be represented as a sum over each electron in the beam:

$$\mathbf{j}e^{-i(\mathbf{kr}-\omega t)} = \sum\nolimits_\alpha \mathbf{v}_\alpha e^{-i(\mathbf{k}_\perp \mathbf{r}_\perp + k_z z - \omega t)}$$

$$\times \delta(\mathbf{r} - \mathbf{r}_\alpha)\theta(t - t_{0\alpha})\theta(T_{0\alpha} - t),$$

where $t_{0\alpha}$ is the moment of time of α-th electron incoming in resonator, $T_{0\alpha}$ is the moment of electron departure from resonator. $\delta(\mathbf{r} - \mathbf{r}_\alpha)$ is δ-function, $\theta(t)$ is θ-function.

Let us average expression (6) over electron phases Θ_0 and Θ_1:

$$I = 2\pi j_0 \Phi \int_0^{2\pi} \frac{d\Theta_1}{2\pi} \int_0^{2\pi} \frac{d\Theta_0}{2\pi} e^{-i\Theta(t,z,\Theta_1-\Theta_0)}, \qquad (7)$$

where $j_0 = en_b u$. This averaging is correct because of law of conservation of particle number which having form:

$$jdt = j_0 dt_0.$$

So, Liouville Theorem of conservation phase volume can be applied. Finally right-hand side of (3) has the following form:

$$I = 2\pi j_0 \Phi \int_0^{2\pi} \frac{2\pi - p}{8\pi^2} \left(\exp(-i\Theta(t, z, p)\right. \qquad (8)$$

$$\left. + \exp(-i\Theta(t, z, -p))\right) dp,$$

Transition from (7) to (8) can be obtain by decomposition of plane figure into integral sums well-known in mathematical analysis.

Numerical methods for solving (3)–(5) and its versions nonlinear stage simulation were proposed [14], [15]. They are implemented in computer code VOLC [17]. Different VFEL geometries were investigated [14]–[19] numerically. All numerical results are in good agreement with analytical predictions and experimental results [11], [8]. The main result of numerical simulations is numerical validation of all main VFEL physical theoretical principles.

3. Steady-state solution

Let us try to obtain solution of the system (3)–(5) on reaching steady-state regime. We find such solution in two-mode form:

$$E = C_1 e^{ik\delta_1 z} + C_2 e^{ik\delta_2 z},$$

$$E_\tau = s_1 C_1 e^{ik\delta_1 z} + s_2 C_2 e^{ik\delta_2 z}, \qquad (9)$$

$$j = j_1 e^{ik\delta_1 z} + j_2 e^{ik\delta_2 z}.$$

Substituting (9) into (3)–(4) we obtain for each mode the following system for roots of dispersion equation δ_n and unknown coefficients C_n and s_n:

$$s_n = \frac{\chi_{-\tau}}{l_1 + 2\gamma_1\delta_n},$$

$$\delta_n = (-(l_1\gamma_0 + l\gamma_1 - \gamma_1\tilde{j}_n) \pm ((l_1\gamma_0 + l\gamma_1$$

$$-\gamma_1\tilde{j}_n)^2 - 4\gamma_0\gamma_1(ll_1 - r - l_1\tilde{j}_n))^{1/2})/(4\gamma_0\gamma_1), \qquad (10)$$

$$C_1 = \frac{-E_0 s_2 e_2}{s_1 e_1 - s_2 e_2}, \quad C_2 = \frac{E_0 s_1 e_1}{s_1 e_1 - s_2 e_2},$$

$$\tilde{j}_n = 2\Phi j_n / C_n, \quad e_n = e^{ik\delta_n L}, \quad r = \chi_\tau \chi_{-\tau},$$
$$n = 1, 2.$$

When $j_n = 0$ we obtain exact solution of two-wave diffraction problem in resonator. If $j_n(t) = const$ then the solution (9) is found stationary. If $j_n(t) \neq const$ solution (10) is not valid. But it allows to treat situation when we deal with smooth reconfiguration of this solution with respect to z and steady-state oscillations with respect to t. In computer animation this looks like as the solution "breathes". In the next section examples of computer simulation illustrate such behavior.

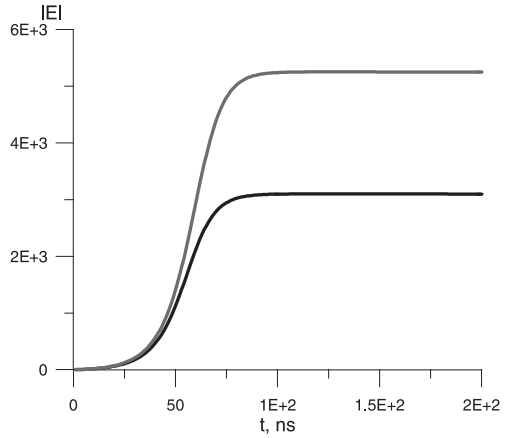

FIG. 2. Time-dependent amplitudes for transmitted (black line) and diffracted (grey line) waves for L=9 cm and j =3 kA/cm^2

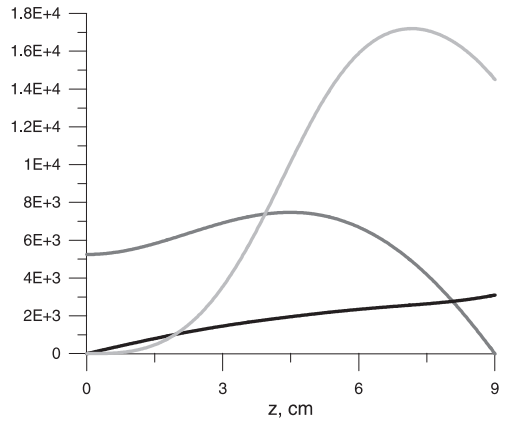

FIG. 3. Amplitudes for transmitted (black line), diffracted (grey line) waves and absolute value of (8) (light grey line) inside the resonator at the last moment of time for L=9 cm and j =3 kA/cm^2.

4. Some numerical results

Investigation of origin of chaos in electronic vacuum devices is very topical in modern physics [13], [20]–[22]. We met with oscillations during VFEL investigation too. In VFEL reasons of initiation of chaotic dynamics remain the same as in other electronic devices: non-uniform distribution of intensity of electromagnetic field and field of spatial charge of electron beam leading to significant perturbations in movement of electrons through resonator. This results to

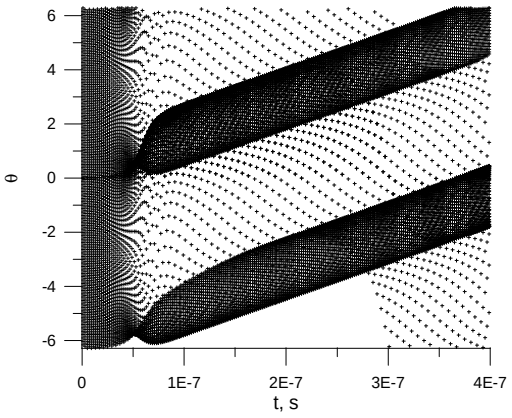

FIG. 4. Time-dependent electron phase in a wave at z=9 cm for L=9 cm and j =3 kA/cm^2.

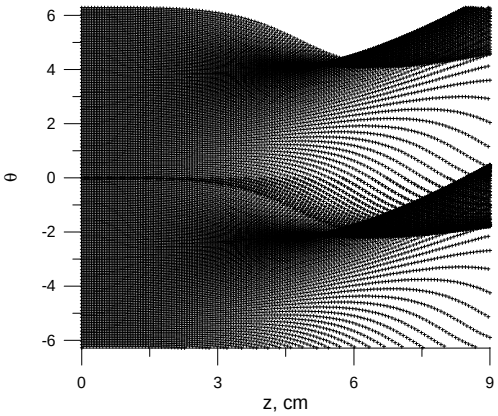

FIG. 5. Electron phase in a wave inside the resonator at the last moment of time for L=9 cm and j =3 kA/cm^2.

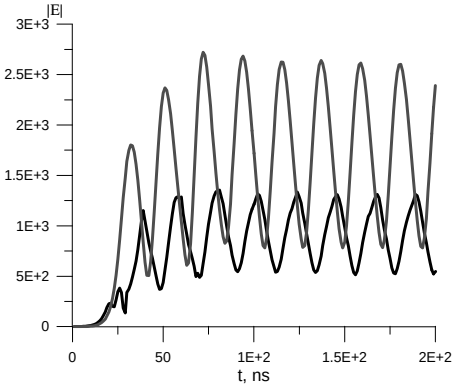

FIG. 6. Time-dependent amplitudes for transmitted (black line) and diffracted (grey line) waves for L=32 cm and j = 500 A/cm^2.

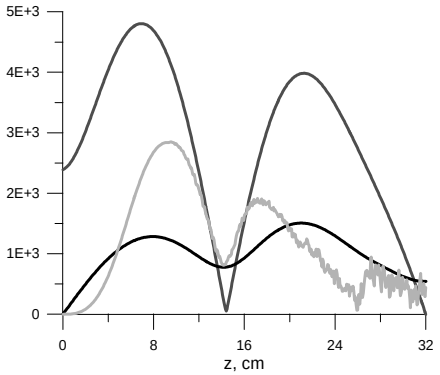

FIG. 7. Amplitudes for transmitted (black line), diffracted (grey line) waves and absolute value of (8) (light grey line) inside the resonator at the last moment of time for L=32 cm and $j = 500$ A/cm^2.

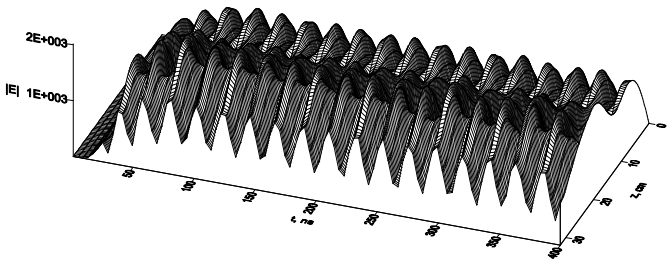

FIG. 8. Time-dependent amplitude for transmitted wave inside the resonator for L=32 cm and j =500 A/cm^2.

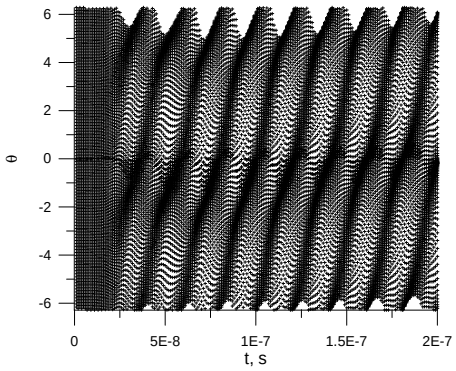

FIG. 9. Time-dependent electron phase in a wave at z=6.5 cm for L=32 cm and $j = 500$ A/cm^2.

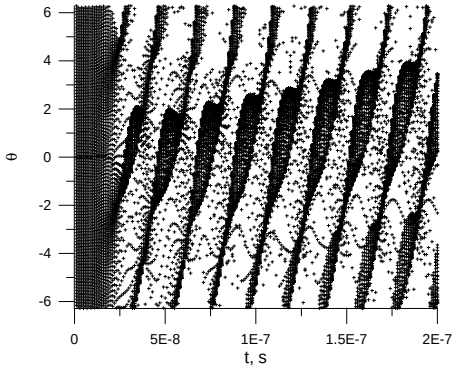

FIG. 10. Time-dependent electron phase in a wave at z=13 cm for L=32 cm and $j = 500$ A/cm^2.

reduction of average velocity of electrons and to deformation of bunches during overtaking some electrons by other ones, to stratification of electron beam etc. The higher harmonics of these fields and their combinations are excited and raised. This leads to chaos in the system.

Investigation of chaos in VFEL is important in the light of experimental development of VFEL. In [15]–[19] a gallery of different chaotic regimes for VFEL laser intensity with corresponding phase space portraits, attractors and Poincaré maps was proposed. There are periodic, quasiperiodic regimes and chaotic self-oscillations. Bifurcation points corresponding to transitions between different regimes of generation were investigated the same as the largest Lyapunov exponents and sensibility of the system behavior to initial conditions. It was analyzed dependence of chaotic lasing on the following couples of parameters: electron beam current and factor of asymmetry, beam current and detuning from exact synchronism condition, beam current and resonator length. Corresponding parametric maps were presented.

Analytical investigation of chaos in VFEL seems to be impossible because of nonlinearity of the system of equations formative VFEL mathematical model. In the paper presented the chaotic behavior in two-wave VFEL amplifier was investigated for the following set of parameters: wavelength $\lambda = 3$ cm, $L = 9$, 20, 32 cm, $j = 500$ and 3000 A/cm^2.

First example is an example of stationary process for $L = 9$ cm and $j = 3$ kA/cm^2. Corresponding plots are presented in Fig. 2 –

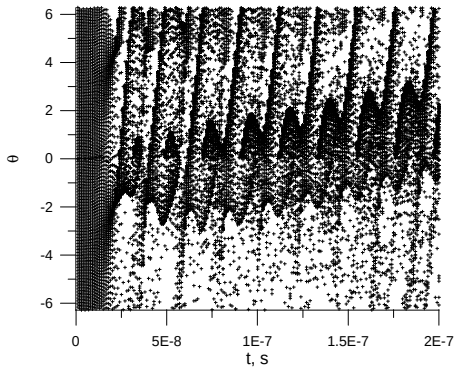

FIG. 11. Time-dependent electron phase in a wave at z=19 cm for L=32 cm and $j = 500$ A/cm^2.

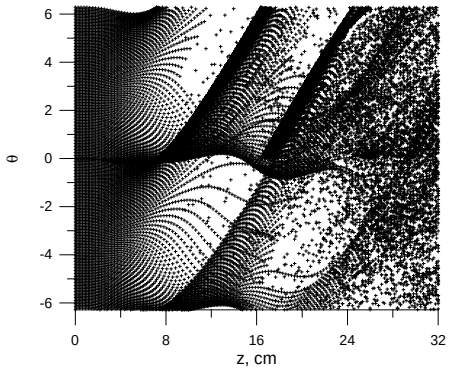

FIG. 12. Electron phase in a wave inside the resonator at the last moment of time for L=32 cm and $j = 500A/cm^2$.

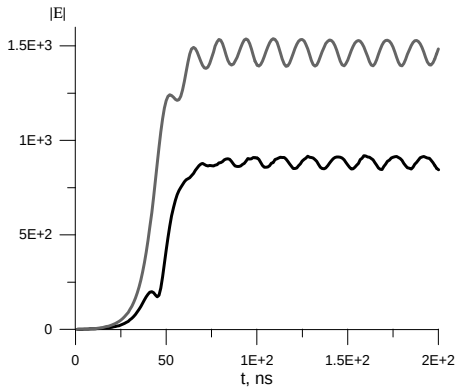

FIG. 13. Time-dependent amplitudes for transmitted (black line) and diffracted (grey line) waves for L=20 cm and $j = 500$ A/cm^2.

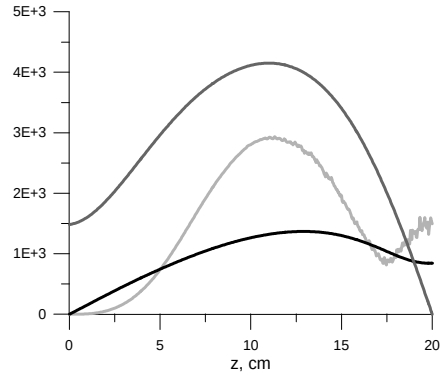

FIG. 14. Amplitudes for transmitted (black line), diffracted (grey line) waves and absolute value of (8) (light grey line) inside the resonator at the last moment of time for L=20 cm and $j = 500$ A/cm^2.

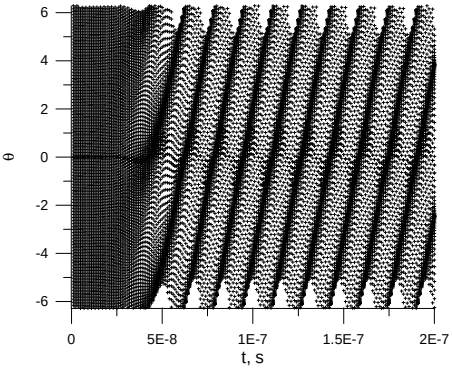

FIG. 15. Time-dependent electron phase in a wave at z=8 cm for L=20 cm and $j = 500$ A/cm^2.

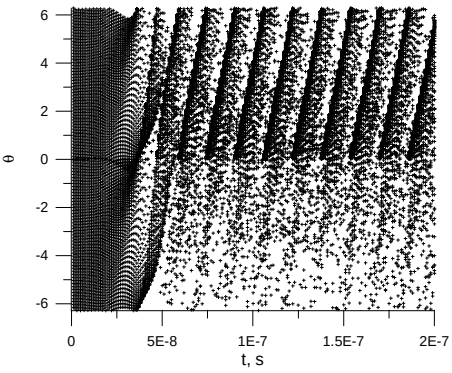

FIG. 16. Time-dependent electron phase in a wave at z=20 cm for L=20 cm and $j = 500$ A/cm^2.

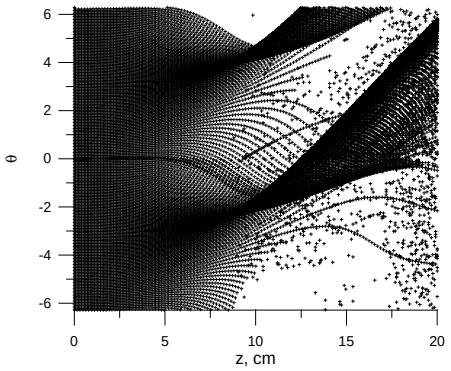

FIG. 17. Electron phase in a wave inside the resonator at the last moment of time for L=20 cm and $j = 500A/cm^2$.

Fig. 5. Time-dependent amplitudes for transmitted and diffracted waves in Fig. 2 demonstrate achievement of steady-state stationary regime. So, if we try to animate in time solution inside the resonator (see Fig. 3) this animation is static (immovable). This is a case $j_n(t) = const$ provided bunching electrons in two bands (structures) with phase shift equal to 2π. This is obvious from Fig. 4 and Fig. 5. In time (Fig. 4) these structures are moving very slowly.

Next simulation was carried out for the following set of parameters: $L = 32$ cm and $j = 500$ A/cm^2. It is depicted in Fig. 6 – Fig. 11. This is an example of large-scale amplitude regime. Description of large-scale and small-scale amplitude regimes were given in [18], [19]. Here this example was chosen to demonstrate electron bunching down to approximately 18 cm (see Fig. 7, 9, 11). Phase structures are changing in time very quickly in comparison with previous example. After that, destruction of these structures passes. Inside resonator electrons bunch in two wide structures that are destroyed further (see Fig. 12). It indicates that electrons gave all possible energy to electromagnetic wave and left wave synchronism. Fig. 7 and Fig. 8 illustrate discussion of previous section that when $j_n(t) \neq const$ solution oscillates.

Fig. 13 – Fig. 17 correspond to parameter set $L = 20$ cm and $j = 500$ A/cm^2. This is an example of small-scale amplitude regime. Here again electrons bunch in time till approximately 17 cm (see Fig. 14, Fig. 15). This fact confirms that effective resonator length for not great beam current is equal approximately to 6 wave lengths [11]. Destruction of bunches begins at exit of resonator (Fig. 16). Inside the resonator two structures are shaped again (Fig. 17). One of them then passes to other. These structures are not so wide as in the case of $L = 32$ cm but not so narrow as in the first case at $L = 9$ cm.

5. Conclusion

Since VFEL physical principles differ from ones using in other electronic vacuum devices we deal with a new subject of inquiry. So, each step in investigation of its nonlinear dynamics will profit some new results.

Investigation of nonlinear dynamics of electron beam instability in VFEL showed the complicated nature of such interaction leading to intricate changing of regimes of operation under changing of control parameters. Full describing of features of such dynamics is extremely laborious because of presence of many control parameters. But such investigations are in progress and will be useful for providing experiments on the installations created at the Research Institute for Nuclear Problems of Belarusian State University.

Investigations presented are attempts to display origin of steady-state stationary and oscillatory VFEL regimes and demonstrates structure of electron bunches originating when electron beam passing through photonic crystal in VFEL.

Author thanks Prof. V. G. Baryshevsky for permanent interest to her work. This work was supported by Belarusian Republican Foundation for Fundamental Research, grant No. F07V-001.

References

[1] D.I. Trubetskov, A.E. Hramov. *Lectures on microwave electronics for physicists* (Fizmatlit, Moscow, 2003)(in Russian).

[2] L.A. Vainshtein, V.A. Solncev. *Lectures on microwave electronics* (Soviet Radio, Moscow, 1973)(in Russian).

[3] T. Marshall. *Free-Electron Laser* (Macmillan Pub. Company, New York, 1985).

[4] V.G. Baryshevsky, I.D. Feranchuk. Parametric beam instability of relativistic charged particles in a crystal. Phys. Let. **A102**, 141-144 (1984).

[5] V.G. Baryshevsky, I.Ya.Dubovskaya, I.D. Feranchuk. Cherenkov instability of beam of relativistic particles moving through three-dimentional periodical structure. Proc. of the Belarusian Nat. Ac. Sci., ser. phys.-mat.sci. **N1**, 92-976 (1988).

[6] V.G. Baryshevsky, K.G. Batrakov, I.Ya. Dubovskaya. Parametric (quasi-Cherenkov) X-ray free electron laser. J. Phys **D24**, 1250-1257 (1991).

[7] V.G. Baryshevsky. Volume free electron laser. Nucl. Instr. Meth. **A445**, 281-283 (2000).

[8] V.G. Baryshevsky, A.A. Gurinovich. Spontaneous and induced parametric and Smith-Purcell radiation from electrons moving in a photonic crystal built from the metallic threads. Nucl. Instr. Meth. **B252**, 92-101 (2006).

[9] V.G. Baryshevsky et al. First lasing of a volume FEL (VFEL) at a wavelength range 4-6 mm. Nucl. Instr. Meth. **A483**, 21-24 (2002).

[10] V.G. Baryshevsky et al. Experimental observation of radiation frequency tuning in OLSE-10 prototype of volume free electron laser. Nucl. Instr. Meth. **B252**, 86-91 (2006).

[11] V.G. Baryshevsky et al. Experimental study of a volume free electron laser with a "grid" resonator. Proc. of FEL 2006, BESSY, 331-333 (2006).

[12] S.L. Chang. *Multiple diffraction of X-rays in crystals* (Springer-Verlag, Berlin, 1984).

[13] S.P. Kuznetsov. Nonlinear dynamics of backward-wave tube: self-modulation, multi-stability, control. Izvestija VUZov - Applied Nonlinear Dynamics. **14**, 3-35 (2006).

[14] K.G. Batrakov, S.N. Sytova. Nonstationary stage of quasi-Cherenkov beam instability in periodical structure. Mathematical Modelling and Analysis. **10**, 1-8 (2005).

[15] K.G. Batrakov, S.N. Sytova. Modelling of Volume Free Electron Lasers. Computational Mathematics and Mathematical Physics. **45**, 666-676 (2005).

[16] K.G. Batrakov, S.N. Sytova. Dynamics of electron beam instabilities under conditions of multiwave distributed feedback. Nonlinear Phenomena in Complex Systems. **8**, 359-365 (2005).

[17] K.G. Batrakov, S.N. Sytova. Mathematical modeling of multiwave Volume Free Electron Laser: basic principles and numerical experiments. Mathematical Modelling and Analysis. **11** 13–22 (2006).

[18] S.N. Sytova. Numerical Analysis of Lasing Dynamics in Volume Free Electron Laser. Mathematical Modelling and Analysis. **13**, 263-274 (2008).

[19] S.N. Sytova. Volume Free Electron Laser (VFEL) as a dynamical system. Nonlinear Phenomena in Complex Systems. **10**, 297-302 (2007).

[20] C. Bruni, D. Garzella et al. Chaotic nature of the super-ACO FEL. Nucl. Instr. Meth. **A528**, 273-277 (2004).

[21] N.M. Ryskin. Study of the nonlinear dynamics of a travelling-wave-tube oscillator with delayed feedback. Radiophysics and Quantum Electronics. **47**, 116-128 (2004).

[22] H.J. Lee, J.K. Lee et al. A universal characterization of nonlinear self-oscillation and chaos in particle-wave-wall interactions. Appl. Phys. Let. **72**, 1445-1447 (1998).